Environmental Science & Technology

Article

pubs.acs.org/est

Comparison of Experimental and Modeled Absorption Enhancement by Black Carbon (BC) Cored Polydisperse Aerosols under Hygroscopic Conditions

P. M. Shamjad,[†] S. N. Tripathi,*[,†] S. G. Aggarwal,[‡] S. K. Mishra,[‡] Manish Joshi,[§] Arshad Khan,[§] B. K. Sapra,[§] and Kirpa Ram[∥]

[†]Department of Civil Engineering, Indian Institute of Technology, Kanpur, India

[‡]CSIR, National Physical Laboratory, New Delhi, India

[§]Radiological Physics and Advisory Division, Bhabha Atomic Research Centre, Mumbai, India

[∥]Department of Earth and Planetary Science, Graduate School of Science, University of Tokyo, Japan

ABSTRACT: The quantification of the radiative impacts of light absorbing ambient black carbon (BC) particles strongly depends on accurate measurements of BC mass concentration and absorption coefficient (β_{abs}). In this study, an experiment has been conducted to quantify the influence of hygroscopic growth of ambient particles on light absorption. Using the hygroscopic growth factor (i.e., Zdanovskii–Stokes–Robinson (ZSR) approach), a model has been developed to predict the chemical composition of particles based on measurements, and the absorption and scattering coefficients are derived using a core–shell assumption with light extinction estimates based on Mie theory. The estimated optical properties agree within 7% for absorption coefficient and 30% for scattering coefficient with that of measured values. The enhancement of absorption is found to vary according to the thickness of the shell and BC mass, with a maximum of 2.3 for a shell thickness of 18 nm for the particles. The findings of this study underline the importance of considering aerosol-mixing states while calculating their radiative forcing.

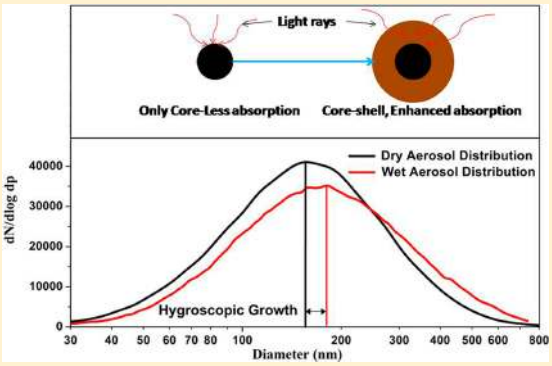

1. INTRODUCTION

Aerosols are known to impact climate in several ways. They can alter the scattering and absorption of solar radiation (direct effect), can cause atmospheric heating by absorption of radiation thus suppressing the convection and reducing cloud cover (semidirect effect), and can affect the formation and properties of clouds by acting as cloud condensation nuclei (indirect effect).[1,2] These effects are estimated by studying the aerosol composition and size distribution which in turn governs the optical and physical properties of composite aerosols.[3] However, significant uncertainties are introduced in these estimations due to dependencies on aerosol size, hygroscopicity, morphology, mixing state, refractive index, and solubility. For example, black carbon (BC) content in the atmospheric aerosols is of great importance due to its highly absorbing nature.[4,5] The estimation of its radiative impact strongly depends on the accurate measurement of absorption coefficient, BC mass concentration, and its mixing state.[5] Internal mixing models of BC (homogeneous or a core–shell structure) show more realistic absorption estimates as compared to external mixing models in which BC particles coexist with other particles in a physically separated manner. It has also been shown that absorption by BC increases when BC particles are mixed and/or coated with other less absorbing materials.[6] This enhanced absorption in a core–shell structure is because of the focusing effect of coated materials (shell) which act as a lens.[7,8]

Enhanced absorption is mainly brought about by high atmospheric relative humidity (RH) in the presence of high levels of nonabsorbing hygroscopic aerosols such as sulfates (SO_4^{2-}), nitrates (NO_3^-), and water-soluble organic carbon (WSOC), as their hygroscopic nature favors internal mixing/core–shell formation. Nessler et al.[9] have reported an enhancement of up to 53% in aerosol absorption as RH increased from 0% to 99%. Such conditions prevail in the Indo-Gangetic Plain (IGP) during wintertime when the entire region is characterized by the presence of high levels of BC and hygroscopic materials.[10−12] In such a case, the coating of hygroscopic materials on BC core and internal mixing is a plausible mechanism for explaining the 5-fold enhancement observed in the optical BC mass concentrations (in other words absorption coefficient) in a recent study.[13]

The objective of the current study is to calculate the hygroscopic growth of aerosols during winter season (December–February) over an urban site (Kanpur) in the

Received: January 26, 2012
Revised: July 9, 2012
Accepted: July 12, 2012

   dx.doi.org/10.1021/es300295v | Environ. Sci. Technol. XXXX, XXX, XXX–XXX

IGP and thereby explain the enhancement in BC absorption coefficient. A laboratory experiment was set up to quantify the hygroscopic growth of particles using two scanning mobility particle sizers (SMPSs) operating in parallel[14] for 5 days in winter season of February 2011. An internal mixing state with black carbon particles forming a concentric core−shell structure with other hygroscopic and less absorbing particles was assumed. Volume fractions of different chemical species were calculated using a model developed by considering individual hygroscopicity and bulk hygroscopic growth. The individual volume fractions were then used to calculate the refractive indices of the core and shell separately. These parameters along with the measured size distribution were fed into the code developed by Dr. W. Wiscombe, based on the work reported by Toon and Ackerman[15] to compute the scattering and absorption by concentric spheres. Results from this code were compared with the experimental values measured during the study period.

We also have measured the absorption and black carbon for four consecutive winter seasons (2007−2010). Our analysis shows that hygroscopic growth of particles is a likely cause for the varying degree of enhancement in absorption for the same BC mass during winter seasons in each year as demonstrated in 2011 experiment.

2. EXPERIMENTAL SECTION

The experimental study was carried out on the campus of Indian Institute of Technology which is located in the city of Kanpur, (26.5° N, 80.3° E, 142 m msl), in the IGP. It has a large urban population of around 2.6 million. The pollution sources in the region are of mixed origin which includes domestic, industrial, and vehicular emissions.[16] During winter season, heavy fog and haze are observed in the entire IGP.[17,18] All measurements of atmospheric aerosols were carried out at a height of 5 m from the ground level. Hourly averaged atmospheric RH was also measured using an automatic weather station (AWS) located inside the campus.

Measurement of BC and Optical Properties. An Aethalometer (AE-31, Magee Scientific) was used for the measurement of BC mass in seven wavelengths, at 370, 470, 520, 590, 660, 880, and 950 nm with a flow rate of 2 L min^{-1}. More details about the Aethalometer are described elsewhere.[17] The instrument was kept inside the laboratory and a tube (made of rubber with a conductive material coating inside) 1 m long and 0.3 cm in diameter was used for ambient aerosol sampling. The data were collected every 5 min and corrections were applied for both shadowing effect which is negligible for atmospheric aerosols[19]and multiple scattering effects as suggested by Coen et al.[20] Ambient RH varied from 59 to 76.5% during the study period. During wintertime, foggy conditions prevail in IGP, which may lead to even higher RH and sometimes saturation. It has been suggested that high RH conditions up to 85% did not have significant effect on Aethalometer-measured BC mass as was shown in Schmid et al.[21] Thus, Aethalometer BC measurement is expected to be least affected by the ambient RH condition. In addition, the inside temperature of the laboratory was always higher than the ambient through the entire sampling duration thus inhibiting the condensation of droplets on the Aethalometer which can cause errors.

Absorption coefficient (β_{abs_exp}) and scattering coefficient (β_{scat_exp}) were measured using a photoacoustic soot spectrometer[22] (PASS-1, Droplet Measurement Technologies). The details about the measurements of absorption and scattering coefficients by PASS-1 are described in a recent publication.[23] PASS-1 records data every second and the average for every 5-min interval is reported here at a single wavelength, 781 nm. It has been noticed that PASS-1 measured absorption shows a systematic reduction when the RH increases beyond 70% due to influence of mass transfer to the theoretical photoacoustic signal.[22] The measured absorption coefficient in this study is corrected by linearly extrapolating the curve up to 100% RH in the Figure 8 of Arnott et al.[22] Since the PASS-1 operates at a single wavelength of 781 nm, the Aethalometer BC mass between 660 and 880 nm was linearly interpolated to estimate the value at 781 nm so that the data from the two instruments could be compared.

Hygroscopic Growth. Hygroscopicity is the parameter that describes the interaction of atmospheric particles with water vapor and is generally measured using a hygroscopic tandem differential mobility analyzer (H-TDMA).[24,25] Alternatively, hygroscopic growth can also be estimated by comparing ambient (wet) and dry particle size distributions obtained using two SMPSs operating in parallel approach[14] as

$$g_{\exp} = \frac{d_{m,wet}}{d_{m,dry}} \quad (1)$$

where $d_{m,wet}$ is the mode diameter of the ambient size distribution (wet) and $d_{m,dry}$ is that of the corresponding dry size distribution.

The size distributions were measured using a SMPS which included a differential mobility analyzer (DMA), which segregates particles according to their mobility in an applied electric field, and a condensation particle counter (CPC), which counts the particles in a given mobility range. The mobility distribution thus estimated is converted to the size distribution through an inversion algorithm. Following the approach suggested in eq 1, the ambient size distribution was measured using the TSI (model 3696) SMPS. The dry distribution was measured using a Grimm (model 5.403) SMPS which had a dryer attached to its inlet to remove the water content from the atmospheric aerosols. The dryer used contained silica beads which remove water content of the ambient aerosol reducing RH to below 5%. These silica beads were regenerated every day by drying at 180 °C for 2 h in an oven. Both SMPSs were operated with a sheath flow of 3.0 L min^{-1} and a sample flow of 0.3 L min^{-1}. The total sampling tube length was maintained at 0.7 m and the scan time was fixed at 7 min 36 s for both instruments. Eight consecutive scan data were averaged to get hourly averaged distributions from both SMPSs. A total of 33 h of data collected during the period of February 5−10, 2011 was used in this study. Atmospheric RH was measured using Vaisala Humidcap (HMT 330, Serial No. B4050039) with an accuracy of 1% for RH < 90% and 1.7% above 90%. In addition, RH at the inlet and outlet of TSI SMPS which was operated for the measurement of size distribution of ambient particles was measured for initial hours of the experiment. The schematic of the experimental arrangement is shown in Figure 1

Initially, as an intercomparison, the particle size-distributions measured by the two SMPSs under similar ambient conditions are depicted in Figure 2a.The mode diameters were within 3%, while the geometric standard deviation was within 1%. Subsequently, ambient and dry particle size-distributions were measured and a clear difference in the mode diameters was seen. Figure 2b−e show such dry and ambient size distributions

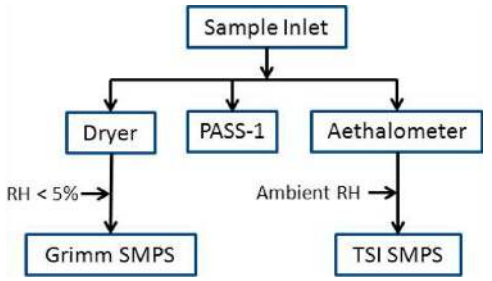

Figure 1. Schematic of experimental setup.

as obtained by the GRIMM and the TSI SMPSs, respectively, at different RH conditions observed during the sampling period. Hourly average mode diameters of size-distributions (dry and ambient conditions) were calculated and the growth factors were derived using eq 1. The growth factors were found to range from 1.02 to 1.18 for RH varying between 59.3 and 76.5%.

3. MODELING

The approach of estimating the chemical composition based on the growth factor of the particles at a given RH is followed here.[26,27] The method of Kreidenweis et al.[26] was used to calculate the individual wet volume fractions (ε_{i_wet}) of each component present in the aerosol. We assume an aerosol system consisting of water-insoluble organic carbon (WISOC), water-soluble organic carbon (WSOC), and inorganic species, i.e. $(NH_4)_2SO_4$ and NH_4NO_3 along with BC. Dust is excluded from the assumed composition because earlier studies had shown negligible presence of dust in Kanpur during the winter season.[18] The bulk hygroscopicity of the mixture ($k_{mixture}$) based on Zdanovskii–Stokes–Robinson (ZSR) approach[28,29] is calculated as

$$k_{mixture} = \sum_i \varepsilon_{i.dry} k_i \quad (2)$$

where ε_{i_dry} is the dry volume fraction and k_i is the hygroscopicity of each individual species present in the aerosol (Table 1). Hygroscopicity is defined as the amount of water absorbed by a particle with a given dry diameter at a given

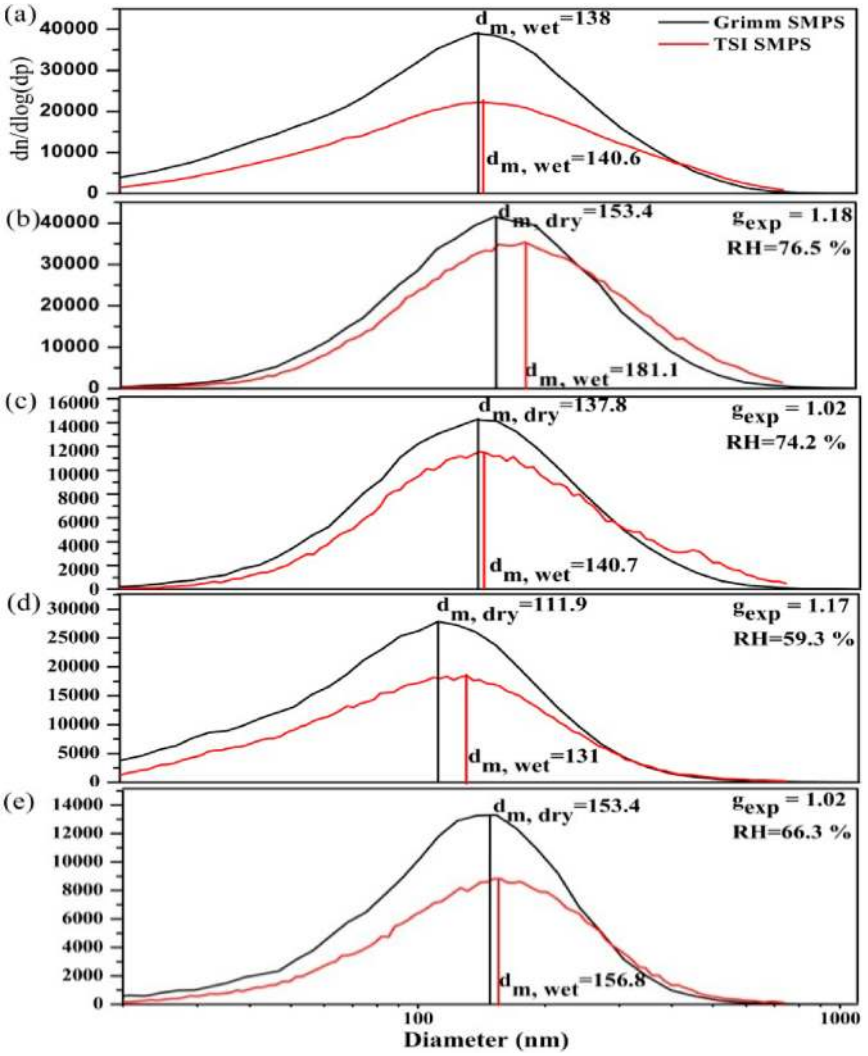

Figure 2. Aerosol size distribution measured by Grimm SMPS and TSI SMPS for (a) similar ambient conditions (b–e) with GRIMM SMPS connected with a dryer for RH =76.5, 74.2, 59.3, and 66.3%, respectively. $d_{m,dry}$ and $d_{m,wet}$ are dry and wet mode diameters, respectively, and g_{exp} is the growth factor.

dx.doi.org/10.1021/es300295v | Environ. Sci. Technol. XXXX, XXX, XXX–XXX

Table 1. Hygroscopicity and Refractive Index of Species Considered in the Study

species	hygroscopicity (k_i)	refractive index	
		real (n)	imaginary (k)
WISOC	0[a]	1.53[c]	0.0131[c]
WSOC	0.15[b]	1.53[c]	0.0032[c]
$(NH_4)_2SO_4$	0.5[b]	1.40[d]	0.60×10^{-7}[d]
NH_4NO_3	0.68[b]	1.40[d]	0.25×10^{-7}[d]
BC	0[a]	1.85[e]	0.75[f]

[a]Because WISOC and BC are insoluble in nature, their $k = 0$. [b]Data from Kreidenweis et al.[26] [c]Data from Arola et al.[38] [d]Data from Bauer et al.[39] [e]Data from Bond and Bergstrom et al.[4] [f]Data from Kirchstetter et al.[40] Refractive indices are selected at wavelengths closest to 781 nm.

RH.[30] The ratio of volume fraction of hydrated water to solid phase aerosol, $((V_w)/(V_s))$ is incorporated in the model using the following relationship

$$\frac{V_w}{V_s} = k_{mixture}\frac{a_w}{1 - a_w} \tag{3}$$

where a_w is the fractional ambient relative humidity (= RH/100) and V_w and V_s are volume of water in aerosol and volume of dry aerosol, respectively.

The modeled hygroscopic growth factor g_{model} is then calculated as

$$g_{model} = \left(\frac{V_w}{V_s} + 1\right)^{1/3} \tag{4}$$

Compositional models with varying fractions of the constituents in aerosol were developed for each hourly SMPS distribution using eqs 2, 3, and 4. For each of these compositions, the difference between the measured and modeled hygroscopic growth factor, i.e. absolute$(g_{exp} - g_{model})$ was estimated. The composition for which this difference was less than 0.5% was accepted. The volume fraction of each component under ambient condition (wet environment) ε_{i_wet} was then estimated as

$$\varepsilon_{i.wet} = \frac{\varepsilon_{i,dry}}{\left(\frac{V_w}{V_s} + 1\right)} \tag{5}$$

Table 2 shows the variation in the volume fractions of each species with cases of RH and growth factors shown in Figure 2b–e. The BC volume fractions thus obtained were converted to BC mass concentration (using average aerosol mass derived from the measured distributions from two SMPSs) assuming a density of 1.8 g cm^{-3} for BC while a density of 1.6 g cm^{-3} is assumed for composite aerosol.[4] Modeled BC concentrations were found to be within 15% of that measured by Aethalometer. This difference is attributable to the fact that the modeled BC considers particle diameters up to one micrometer only as this is the upper cutoff of the SMPSs. On the other hand, the Aethalometer measured the BC mass from all sizes of particles in the atmosphere. The modeled volume fractions of $(NH_4)_2SO_4$ and NH_4NO_3 are compared with those measured by Kaul et al.[16] for winter season of 2009 at Kanpur. A maximum difference of 22% and a minimum difference of 8% are found between modeled and measured volume fractions. These comparisons show that the model developed for the present study reflects the composition, which is close to the actual measured aerosol composition.

Table 2. Change in Modeled Species Volume Fractions with RH and Hygroscopic Growth for the Cases Shown in Figure 2b–e

RH (%)	g_{exp}	volume fractions from hygroscopic model				
		WISOC	WSOC	$(NH_4)_2SO_4$	NH_4NO_3	BC
76.5	1.18	0.485	0.1	0.3	0.05	0.065
74.2	1.02	0.88	0.02	0.02	0.02	0.06
59.3	1.17	0.163	0.2	0.15	0.44	0.048
66.3	1.02	0.89	0.025	0.025	0.025	0.035

Estimation of Optical Parameters. For estimation of scattering and absorption coefficients, an internally mixed concentric core–shell model was considered for which the knowledge of an exact composition of the core and the shell is very important. To arrive at an optimum composition, different combinations of core and shell were tried. When the core is assumed to be of BC only with WISOC, WSOC, and other inorganics as the shell constituents, the refractive index of the model particle (core–shell) was found to be higher. This resulted in higher β_{abs_model} and β_{scat_model} in comparison with the experimental values and hence this compositional model was discarded. The model wherein the core is assumed as a mixture of all species (BC, WISOC, WSOC, $(NH_4)_2SO_4$, and NH_4NO_3) in the dry state and shell as a mixture of soluble species (WSOC, $(NH_4)_2SO_4$, and NH_4NO_3) with water content was considered to be more reasonable.

Major inputs to the code for estimating the optical parameters were the wavenumber, radii of core and shell, and their refractive indices. The wavenumber is defined as $(2\pi/\lambda)$ where λ (= 0.781 μm) is the wavelength at which the calculations are performed. The dry diameter (measured by Grimm SMPS) was taken as core diameter, whereas the shell diameter was calculated by adding shell thickness to the core diameter.The shell thickness was calculated as follows:

$$\text{Shell thickness} = \frac{(d_{m,wet} - d_{m,dry})}{2} \tag{6}$$

All calculations were performed on the hourly averaged data set. The refractive indices of core and shell were calculated using volume mixing method,[2] which requires the refractive index of individual species and the wet volume fraction of each species, ε_{i_wet}, as calculated from eq 5. The refractive indices of individual species were adopted from literature and are given in Table 1. The calculated refractive indices of core and shell by volume mixing rule[2] agree within 1% with those calculated using Maxwell Garnet rule.[31] The core–shell code calculates absorption (β_{abs_model}) and scattering (β_{scat_model}) coefficients for a single particle only. To get the parameters for the polydisperse aerosol distribution, the optical properties of individual particles are integrated over the entire size distribution obtained from SMPS. Absorption and scattering coefficients calculated from core–shell code agree within 10% with those calculated from discrete dipole approximation code.[32]

4. RESULTS AND DISCUSSION

Dry and ambient size distributions for the high RH (Figure 2b and c) and low RH (Figure 2d and e) were used to calculate the hygroscopic growth factors of poly dispersed particles which

dx.doi.org/10.1021/es300295v | Environ. Sci. Technol. XXXX, XXX, XXX–XXX

range from 1.02 to 1.18. The change in growth factor is reflected in the model selected for the calculations of optical parameters. It has been found that not only RH but also the presence (or absence) of hygroscopic species are responsible for higher (or lower) hygroscopic growth. An enhanced fraction of species such as $(NH_4)_2SO_4$ and NH_4NO_3 increases the possibility for higher hygroscopic growth of the particles (Table 2). In an earlier study, Nessler et al.[9] reported a hygroscopic growth factor of 1.54 for a 250-nm dry particle at a RH of 85% in winter season at a high-alpine site of Jungfraujoch. On the other hand, Aggarwal et al.[14] reported a hygroscopic growth factor for polydisperse aerosols as 1.09 at 71% RH in Sapporo, Japan. Marine aerosols show more hygroscopic growth compared to inland aerosols. A study conducted by Massling et al.[33] reported a hygroscopic growth factor between 2 and 2.1 for marine air particles in the range of 250 and 350 nm, respectively, at 90% RH.

The hygroscopic growth factor g_{exp} is also compared with that obtained using aerosol inorganic model, AIM (Clegg et al.; http://www.aim.env.uea.ac.uk/aim/model2/model2a.php).[27] In an earlier study, Kreidenweis et al.[26] reported that for individual inorganic species such as $(NH_4)_2SO_4$ and NH_4NO_3, the ratio $((V_w)/(V_s))$ given by AIM is higher by 34% and 33%, respectively, at a RH of 60% as compared to hygroscopic growth based calculation. This increase in $((V_w)/(V_s))$ results in a higher hygroscopic growth factor given by AIM (g_{AIM}). In the present study also, g_{AIM} is higher than g_{exp} by 24% at a RH of 60%. The lower value of g_{exp} is due to the presence of a large fraction of insoluble species in the particles.

Hourly averages of β_{abs_exp} and β_{scat_exp} are compared with modeled values, which have large dependence on the type of mixing.[6] External mixing of BC shows an underprediction in absorption when compared with internal mixing having core−shell structure. The core−shell mixing calculations can lead to a 50% higher direct radiative forcing compared to external mixing.[34] The core−shell type of internal mixing is found to be the most suitable particle structure to explain the atmospheric mixing state in the current study. Optical properties of this type of mixing are also comparable to those observed by aerosol robotic network (AERONET) based observations at Kanpur. In core−shell structure, the core distribution, which is assumed to be composed of homogeneous mixture of all species in dry state, was measured by Grimm SMPS. When this core is exposed to the atmospheric relative humidity, the soluble part mixes with the water vapor and forms a wet shell consisting of WSOC, $(NH_4)_2SO_4$, and NH_4NO_3, etc. This wet aerosol distribution is measured by TSI SMPS. Since the distribution of dry and wet particles measured by the two different SPMSs shows slight variations in the number concentrations, the calculations were carried out with the mean number concentrations measured by both the instruments.

Figure 3a and b show the comparison between modeled and experimental optical parameters. As may be seen, the difference between β_{abs_model} and β_{abs_exp} was less than 7%. However, the difference between modeled and measured scattering coefficient (less than 30%) was higher than that in the case of absorption coefficient. Error analysis has been carried out by introducing error bars in the experimental data (*Y*-axis) using the standard deviation of each hourly data. The total error in the modeled optical parameters was estimated using Standard Taylor's method.[36] The sources of this error are the error in the growth factor g_{model} and in the number concentration. The total errors in modeled results were found to be ±2.67 Mm^{1-} (1

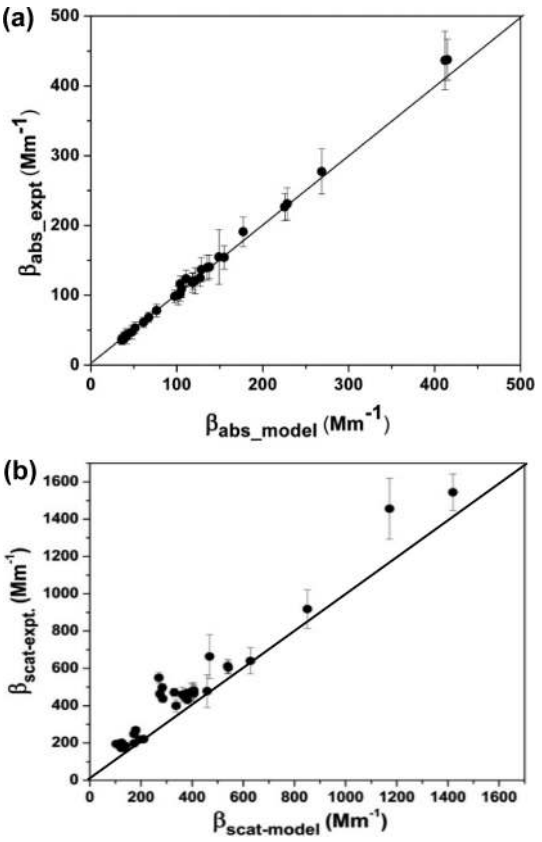

Figure 3. (a) Comparison of β_{abs} obtained from experiment and model calculations. (b) Comparison of β_{scat} obtained from experiment and model calculations.

Mm^{1-} = 10^{-6} m^{-1}) and ±5.72 Mm^{1-} for β_{abs} and β_{scat}, respectively. These values are negligible compared to the error in the experimental data and hence error bars of *X*-axis are not visible in the figures.

In an earlier study conducted by Bond et al.,[6] absorption amplification (γ, defined as the ratio of β_{abs} of core−shell to β_{abs} of core alone) was found to vary from 1.5 to 20 for different monodisperse core and shell configurations. But as in this study, for a polydisperse aerosol system, this enhancement gets reduced due to the damping of cross section oscillations.[9] Another reason for the high γ values in Bond et al.[6] is due to the very high values of shell thickness used in their calculations compared to those observed in the present study. It is observed from the current experiment that the maximum shell thickness due to hygroscopic growth is much less (18 nm).

For the current experimental observations, γ was calculated as the ratio of β_{abs_expt} to β_{abs} due to BC and WISOC which constitute the insoluble core. Core composition is changed to reflect actual atmospheric conditions. In the atmosphere, high RH conditions result in formation of a core−shell structure in which core is constituted of insoluble species (BC + WISOC) and shell with all soluble species and water. Figure 4 in Nessler et al.[2] provides a pictorial representation of core−shell structure considered in this study.The diameter of this insoluble core, $D_{insoluble\_core}$ is calculated from the modeled volume fractions using the equation

$$\frac{D_{insoluble.core}}{D_{dry.core}} = \left(\frac{\varepsilon_{i_{BC}} + \varepsilon_{i_{WISOC}}}{\sum \varepsilon_i}\right)^{1/3} \quad (7)$$

dx.doi.org/10.1021/es300295v | Environ. Sci. Technol. XXXX, XXX, XXX−XXX

where D_{dry_core} is the diameter of dry particle with all species (BC, WISOC, WSOC, $(NH_4)_2SO_4$, and NH_4NO_3) and $\sum\varepsilon_i$ is the sum of volume fractions of individual species which equals to 1.

Figure 4 shows the variation in γ as a function of BC mass fraction and shell thickness. The former is estimated as the ratio

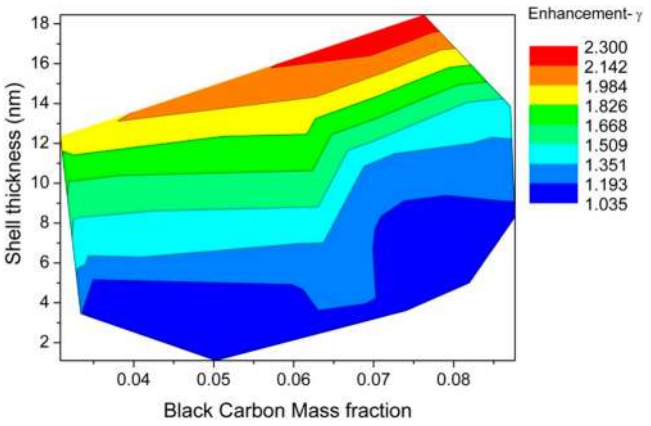

Figure 4. Absorption enhancement as a function of BC mass fraction and shell thickness. Each color shows range of absorption enhancement.

of the BC mass as measured by the Aethalometer to the total mass of particles with an aerodynamic diameter <1 μm as inferred from the SMPS number distribution (assuming a particle density = 1.6 gcm^{-3}). This figure shows a clear trend of increase in γ values as shell thickness increases for a constant BC mass fraction. While a maximum γ of 2.3 is observed for the shell thickness of 18 nm, the lowest γ of 1.035 corresponds to very thin coating (2 nm). It is also seen from this figure that even for very high BC mass fraction, the enhancement in absorption will be predominant only when there is sufficient coating of soluble material (i.e., core−shell thickness >10 nm). In such cases, even a small amount of BC mass fraction (<5%) can produce high absorption. Considering the entire hourly data, an average absorption enhancement of 1.42 is found in the present study.

During the February 2011 experiment β_{abs_exp} and β_{scat_exp} of particles was measured using PASS-1 and BC mass using Aethalometer. Regression analysis of β_{abs_exp} and BC mass (figure not shown) shows a very good correlation (R^2 = 0.98) with higher slope (20.92). This higher slope indicates enhancement in absorption due to hygroscopic growth of particles. Figure 5 shows the linear regression plot between β_{abs_exp} and BC mass for the four winter seasons. Although strong correlations (R^2 = 0.75, 0.71, 0.81, and 0.67 for years 2007, 2008, 2009, and 2010, respectively) are seen, the slopes of the regression lines show large interannual variation for the same season (5.2, 12.6, 18.0, and 23.3, respectively). The higher slope indicates an enhanced β_{abs_exp} measured by PASS-1 for the same BC mass measured by the Aethalometer. Since PASS-1 operates on photoacoustic technique and does not alter the particle structure, it is able to measure the enhanced absorption due to the coating of hygroscopic materials over the black carbon.[37] On the other hand, Aethalometer, being a filter-based method, measures the absorption due to BC. It is quite possible that morphology of ambient aerosols (e.g., core−shell or coating of hygroscopic material) is altered due to impaction on the filter. This means that the enhancement in the absorption

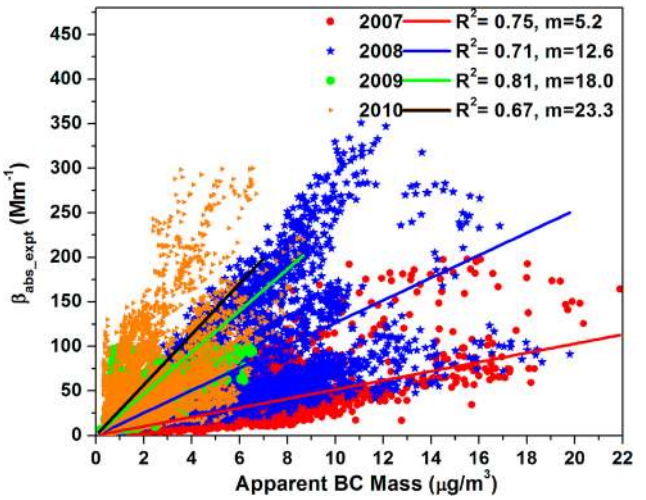

Figure 5. Linear regression analysis between PASS-measured β_{abs} and Aethalometer-measured BC mass for four consecutive winter seasons at Kanpur.

signal is not measured by the Aethalometer and thus it underestimates the true absorption.

Atmospheric RH indicates winter 2007 as a dry period with lower values of RH. The lowest slope for regression line in Figure 5 is seen for this year and the frequency of RH occurring above 70% is less compared to other years. This period also has higher share of lower RH (below 50%) showing dry period, which prevents mixing and/or coating. Winters 2008−2010, which show higher slopes for regression lines, have higher frequency of RH above 70%. This higher RH, combined with hygroscopic species present in the atmosphere, provides a favorable condition for internal mixing of particles for formation of core−shell structure, which may be causing the enhanced absorption measured by PASS-1. February 2011 experiments indicate that high RH alone is not enough to produce enhanced absorption and the presence of inorganic species to form a shell or coating is also an important factor for enhanced absorption.

Findings from this study indicate that the coating of soluble material over black carbon can significantly increase the absorption depending upon the thickness of the coating and type of coating material. High RH conditions and the presence of hygroscopic materials are very much favorable for forming such coatings. Knowledge of easily measurable hygroscopic growth factors can be effectively used to identify the volume fractions of different species present in the ambient aerosol. Using this information in conjunction with the size distribution data, an effective optical closure can be performed to match the experimental optical parameters. Another important finding of this study is that the absorption coefficients estimated based on the Aethalometer data may not be accurate as seen by comparisons with the PASS-1 data.

AUTHOR INFORMATION

Corresponding Author

*E-mail: snt@iitk.ac.in.

Notes

The authors declare no competing financial interest.

■ ACKNOWLEDGMENTS

The present work is supported by a grant under Board of Research in Nuclear Sciences, Department of Atomic Energy. We are thankful to Deepika Bhattu for her help in making the plots. S.N.T. is thankful to Mike Bergin for many helpful discussions.

■ REFERENCES

(1) Intergovernmental Panel on Climate Change (IPCC). *Climate Change 2001. The Scientific Basis*; 2001.

(2) Nessler, R.; Weingartner, E.; Baltensperger, U. Adaptation of Dry Nephelometer Measurements to Ambient Conditions at the Jungfraujoch. *Environ. Sci. Technol.* **2005**, *39* (7), 2219−2228.

(3) Ramana, M. V.; Ramanathan, V.; Feng, Y.; Yoon, S.-C.; Kim, S.-W.; Carmichael, G. R.; Schauer, J. J. Warming influenced by the ratio of black carbon to sulphate and the black-carbon source. *Nat. Geosci.* **2010**, *3*, 542−545.

(4) Bond, T. C.; Bergstrom, R. W. Light absorption by carbonaceous particles: An investigative review. *Aerosol Sci. Technol.* **2006**, *40* (1), 27−67.

(5) Jacobson, M. Z. Strong radiative heating due to the mixing state of black carbon in atmospheric aerosols. *Nature* **2001**, *409* (6821), 695−697.

(6) Bond, T. C.; Habib, G.; Bergstrom, R. W. Limitations in the enhancement of visible light absorption due to mixing state. *J. Geophys. Res.-Atmos.* **2006**, *111*, D20211 DOI: 10.1029/2006JD007315.

(7) Fuller, K. A. Scattering and absorption cross sections of compounded spheres. III. Spheres containing arbitrarily located spherical inhomogeneities. *J. Opt. Soc. Am. A* **1995**, *12*, 893−904.

(8) Fuller, K. A.; Malm, W. C.; Kreidenweis, S. M. Effects of mixing on extinction by carbonaceous particles. *J. Geophys. Res.-Atmos.* **1999**, *104* (D13), 15941−15954.

(9) Nessler, R.; Weingartner, E.; Baltensperger, U. Effect of humidity on aerosol light absorption and its implications for extinction and the single scattering albedo illustrated for a site in the lower free troposphere. *J. Aerosol Sci.* **2005**, *36* (8), 958−972.

(10) Ram, K.; Sarin, M. M. Day-night variability of EC, OC, WSOC and inorganic ions in urban environment of Indo-Gangetic Plain: Implications to secondary aerosol formation. *Atmos. Environ.* **2011**, *45*, 460−468.

(11) Ram, K.; Sarin, M. M.; Tripathi, S. N. A 1 year record of carbonaceous aerosols from an urban location (Kanpur) in the Indo-Gangetic Plain: Characterization, sources and temporal variability. *J. Geophys. Res.* **2010**, *115*, D24313.

(12) Rengarajan, R.; Sarin, M. M.; Sudheer, A. K. Carbonaceous and inorganic species in atmospheric aerosols during wintertime over urban and high-altitude sites in North India. *J. Geophys. Res.* **2007**, *112*, D21307.

(13) Ram, K.; Sarin, M. M.; Tripathi, S. N. Inter-comparison of thermal and optical methods for determination of atmospheric black carbon and attenuation coefficient from an urban location in northern India. *Atmos. Res.* **2010**, *97* (3), 335−342.

(14) Aggarwal, S. G.; Kawamura, K. Determination of aerosol water content under near ambient humidity condition. *Asian Aerosol Conference AAC09, Nov 24−27,* 2009.

(15) Toon, O. B.; Ackerman, T. P. Algorithms for the calculation of scattering by stratified spheres. *Appl. Opt.* **1981**, *20* (20), 3657−3660.

(16) Kaul, D. S.; Gupta, T.; Tripathi, S. N.; Tare, V.; Collett, J. L. Secondary Organic Aerosol: A Comparison between Foggy and Nonfoggy Days. *Environ. Sci. Technol.* **2011**, *45* (17), 7307−7313.

(17) Tripathi, S. N.; Dey, S.; Tare, V.; Satheesh, S. K. Aerosol black carbon radiative forcing at an industrial city in northern India. *Geophys. Res. Lett.* **2005**, *32* (8), L08802.

(18) Singh, R. P.; Dey, S.; Tripathi, S. N.; Tare, V.; Holben, B. Variability of aerosol parameters over Kanpur, northern India. *J. Geophys. Res.-Atmos.* **2004**, *109*, D23206 DOI: 10.1029/2004JD004966.

(19) Weingartner, E.; Saathoff, H.; Schnaiter, M.; Streit, N.; Bitnar, B.; Baltensperger, U. Absorption of light by soot particles: determination of the absorption coefficient by means of aethalometers. *J. Aerosol Sci.* **2003**, *34* (10), 1445−1463.

(20) Coen, M. C.; Weingartner, E.; Apituley, A.; Ceburnis, D.; Fierz-Schmidhauser, R.; Flentje, H.; Henzing, J. S.; Jennings, S. G.; Moerman, M.; Petzold, A.; Schmid, O.; Baltensperger, U. Minimizing light absorption measurement artifacts of the Aethalometer: evaluation of five correction algorithms. *Atmos. Meas. Tech.* **2010**, *3* (2), 457−474.

(21) Schmid, O.; Artaxo, P.; Arnott, W. P.; Chand, D.; Gatti, L. V.; Frank, G. P.; Hoffer, A.; Schnaiter, M.; Andreae, M. O. Spectral light absorption by ambient aerosols influenced by biomass burning in the Amazon Basin. I: Comparison and field calibration of absorption measurement techniques. *Atmos. Chem. Phys.* **2006**, *6*, 3443−3462.

(22) Arnott, W. P.; Moosmuller, H.; Rogers, C. F.; Jin, T. F.; Bruch, R. Photoacoustic spectrometer for measuring light absorption by aerosol: instrument description. *Atmos. Environ.* **1999**, *33* (17), 2845−2852.

(23) Jai Devi, J.; Tripathi, S. N.; Gupta, T.; Singh, B. N.; Gopalakrishnan, V.; Dey, S. Observation-based 3-D view of aerosol radiative properties over Indian Continental Tropical Convergence Zone: Implications to regional climate. *Tellus B* **2011**, *63* (5), 971−989.

(24) Swietlicki, E.; Hansson, H. C.; Hameri, K.; Svenningsson, B.; Massling, A.; McFiggans, G.; McMurry, P. H.; Petaja, T.; Tunved, P.; Gysel, M.; Topping, D.; Weingartner, E.; Baltensperger, U.; Rissler, J.; Wiedensohler, A.; Kulmala, M. Hygroscopic properties of submicrometer atmospheric aerosol particles measured with H-TDMA instruments in various environments - a review. *Tellus Ser. B* **2008**, *60* (3), 432−469.

(25) Aggarwal, S. G.; Mochida, M.; Kitamori, Y.; Kawamura, K. Chemical Closure Study on Hygroscopic Properties of Urban Aerosol Particles in Sapporo, Japan. *Environ. Sci. Technol.* **2007**, *41* (20), 6920−6925.

(26) Kreidenweis, S. M.; Petters, M. D.; DeMott, P. J. Single-parameter estimates of aerosol water content. *Environ. Res. Lett.* **2008**, *3*, 3.

(27) Clegg, S. L.; Brimblecombe, P.; Wexler, A. S. Thermodynamic model of the system H^+-NH_4^+-SO_4^{2-}-NO_3^--H_2O at tropospheric temperatures. *J. Phys. Chem. A* **1998**, *102* (12), 2137−2154.

(28) Stokes, R. H.; Robinson, R. A. Interactions in Aqueous Nonelectrolyte Solutions. I. Solute-Solvent Equilibria. *J. Phys. Chem.* **1966**, *70* (7), 2126−2131.

(29) Flores, J. M.; Bar-Or, R. Z.; Bluvshtein, N.; Abo-Riziq, A.; Kostinski, A.; Borrmann, S.; Koren, I.; Rudich, Y. Absorbing aerosols at high relative humidity: closure between hygroscopic growth and optical properties. *Atmos. Chem. Phys* **2012**, 1019−1052.

(30) Ruehl, C. R.; Chuang, P. Y.; Nenes, A. Aerosol hygroscopicity at high (99 to 100%) relative humidities. *Atmos. Chem. Phys.* **2010**, *10* (3), 1329−1344.

(31) Garnett, J. C. M. Colours in Metal Glasses and in Metallic Films. *Philos. Trans. R. Soc. London, A* **1904**, *203*, 385−420.

(32) Draine, B. T.; Flatau, P. J. *User Guide for the Discrete Dipole Approximation Code DDSCAT 6.1*; 2004.

(33) Massling, A.; Leinert, S.; Wiedensohler, A.; Covert, D. Hygroscopic growth of sub-micrometer and one-micrometer aerosol particles measured during ACE-Asia. *Atmos. Chem. Phys.* **2007**, *7* (12), 3249−3259.

(34) Jacobson, M. Z. A physically-based treatment of elemental carbon optics: Implications for global direct forcing of aerosols. *Geophys. Res. Lett.* **2000**, *27* (2), 217−220.

(35) Dey, S.; Tripathi, S. N.; Mishra, S. K. Probable mixing state of aerosols in the Indo-Gangetic Basin, northern India. *Geophys. Res. Lett.* **2008**, *35*, 3.

(36) Taylor, J. R. *An Introduction to Error Analysis: The Study of Uncertainties in Physical Measurements*; University Science Books, 1997.

(37) Shiraiwa, M.; Kondo, Y.; Iwamoto, T.; Kita, K. Amplification of Light Absorption of Black Carbon by Organic Coating. *Aerosol Sci. Technol.* **2010**, *44* (1), 46−54.

(38) Arola, A.; Schuster, G.; Myhre, G.; Kazadzis, S.; Dey, S.; Tripathi, S. N. Inferring absorbing organic carbon content from AERONET data. *Atmos. Chem. Phys.* **2011**, *11* (1), 215−225.
(39) Bauer, S. E.; Mishchenko, M. I.; Lacis, A. A.; Zhang, S.; Perlwitz, J.; Metzger, S. M. Do sulfate and nitrate coatings on mineral dust have important effects on radiative properties and climate modeling? *J. Geophys. Res.-Atmos.* **2007**, *112*, D06307 DOI: 10.1029/2005JD006977.
(40) Kirchstetter, T. W.; Novakov, T.; Hobbs, P. V. Evidence that the spectral dependence of light absorption by aerosols is affected by organic carbon. *J. Geophys. Res.-Atmos.* **2004**, *109*, D21208 DOI: 10.1029/2004JD004999.